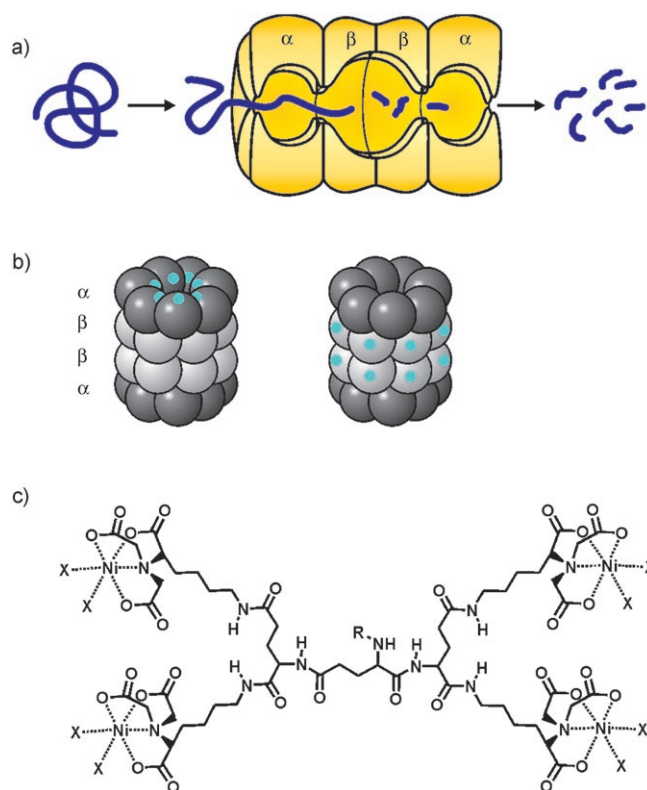


# Controlling the Activity of the 20S Proteasome Complex by Synthetic Gatekeepers\*\*

Katrin Schulze, Alart Mulder, Ali Tinazli, and Robert Tampé\*

The 26S proteasome complex is the central degradation machinery in eukaryotic cells. It is composed of a proteolytically active core complex, the 20S proteasome, and the 19S or 11S regulatory particles (RPs). Within the ubiquitin–proteasome pathway, the proteasome complex is responsible for the degradation of unwanted and malfunctioning proteins.<sup>[1]</sup> It regulates a variety of key cellular processes, such as transcription, signal transduction, and apoptosis, and is involved in tumor development.

Four stacked heptameric rings ( $\alpha_7\beta_7\beta_7\alpha_7$ ) enclosing three nanocompartments make up the 700-kDa barrel-shaped architecture of the 20S proteasome. The central degradation chamber is built up by two inner rings, each containing seven  $\beta$  subunits. The two outer rings consisting of seven closely packed  $\alpha$  subunits give rise to two antechambers (Scheme 1a).<sup>[2]</sup> Substrate entry into this multicatalytic enzyme complex is suggested to be gated by the N-terminal tails of the  $\alpha$  subunits. In the latent state, these N-terminal tails are anchored by an intricate lattice of interactions that restrict substrate entry through the orifices at both ends of the proteasome complex. The N-terminal tails are only a partial barrier to the passage of protein substrates as the restriction is not sufficient enough to hamper the entrance and degradation of short polypeptides.<sup>[3]</sup> These apertures open after association with RPs, like PA700, PA28, or PAN, that render the



**Scheme 1.** a) Substrate degradation by the 20S proteasome complex. Proteins are degraded inside the 20S proteasome complex and peptides are released. Substrate entry as well as product exit occur at both apertures of the proteasome. Access to the complex is controlled by the N-terminal tails of the  $\alpha$  subunits. b) His tags (turquoise) were introduced either at the N termini of the  $\alpha$  subunits ( $\alpha$ N His<sub>6</sub>–proteasome, left) or at the C termini of the  $\beta$  subunits ( $\beta$ C His<sub>6</sub>–proteasome, right) of the 20S proteasome from *T. acidophilum*. c) Chemical structure of the nickel(II)-loaded tetrakisNTA. R = H, carboxyfluorescein, or ATTO565; X = free coordination site occupied by water or histidine.

complex active and enable the processive degradation of proteins.<sup>[4,5]</sup>

The N-terminal tails of the archaeal  $\alpha$  subunits are unstructured, allowing substrate access through ca. 13-Å large entrances even without special regulators.<sup>[6]</sup> The importance of each of these two orifices as both entry and exit gates has been demonstrated by breaking the  $D_7$  symmetry of the 20S proteasome from *Thermoplasma acidophilum* by site-specific, uniformly oriented immobilization at nitrilotriacetic acid (NTA) interfaces.<sup>[7]</sup>

Herein, we present the use of a small synthetic gatekeeper to specifically and reversibly control the proteolytic activity of the 20S proteasome complex. A multivalent chelator head (MCH) with four NTA moieties (tetrakisNTA, Scheme 1c) is used to crosslink His tags introduced either at the N-terminal tails of the  $\alpha$  subunits around the two openings ( $\alpha$ N His<sub>6</sub>–proteasome) or at the C-termini of the  $\beta$  subunits located at the side of the proteasome ( $\beta$ C His<sub>6</sub>–proteasome, Scheme 1b).<sup>[8]</sup> The MCH is able to complex multiple histidine residues at its nickel(II) centers and forms strong, nanomolar-affinity complexes with histidine tags.<sup>[9]</sup>

[\*] K. Schulze, Dr. A. Mulder, A. Tinazli, Prof. R. Tampé  
Institute of Biochemistry, Biocenter  
Johann Wolfgang Goethe-University  
Max-von-Laue-Strasse 9, 60438 Frankfurt a. M. (Germany)  
Fax: (+49) 69-798-29495  
E-mail: tampe@em.uni-frankfurt.de

[\*\*] We would like to thank Drs. Silke Hutschenreiter, Suman Lata and Jacob Piehler for useful discussions and support as well as Gerhard Spatz-Kümbel for excellent technical assistance. The Deutsche Forschungsgemeinschaft (DFG) and the Bundesministerium für Bildung und Forschung (BMBF) supported this research.

We first analyzed the binding of fluorescent tetrakisNTA to the 20S proteasome from *T. acidophilum* by gel filtration chromatography. The  $\alpha$ N His<sub>6</sub>-proteasome was eluted with a retention volume ( $V_R$ ) of 1.44 mL ( $\approx$  700 kDa, Figure 1 a).

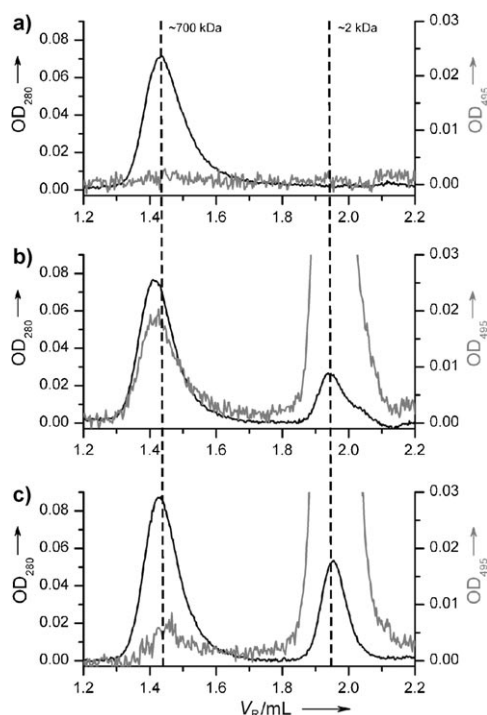


**Figure 1.** Stable complex formation of tetrakisNTA (fluorescein) with the 20S proteasome from *T. acidophilum* analyzed by gel filtration.  $\alpha$ N His<sub>6</sub>-proteasome without a) and with b) 10-fold molar excess of tetrakisNTA (fluorescein). c) Isolation of the released 20S proteasome by addition of imidazole (50 mM) to the running buffer solution. The absorbance was monitored at 280 nm (black) and 495 nm (gray).

After incubation with a 10-fold molar excess of tetrakisNTA (fluorescein), the 20S proteasome elution peak at an optical density (OD) of 280 nm shows coinciding absorbance with 495 nm and a shift to a slightly lower  $V_R$  (1.41 mL), indicating stable complex formation. Free tetrakisNTA (fluorescein) elutes at a  $V_R$  of 1.94 mL ( $\approx$  2 kDa, Figure 1 b). No labeling was observed for proteins without histidine tags<sup>[10]</sup> or in the presence of ethylenediamine tetraacetate (EDTA<sup>2-</sup>; 10 mM) or imidazole (100 mM), demonstrating that MCH binding is site specific. Near-complete dissociation (70–80%) of the MCHs–proteasome complex is achieved upon exposure to imidazole (50 mM), demonstrating the reversibility of the interaction (Figure 1 c). Similar results were obtained for the  $\beta$ C His<sub>6</sub>-proteasome (data not shown).

The number of MCHs bound to the isolated proteasome complexes was determined through the characteristic absorbance of the attached fluorophore and the protein concentration by using a bicinchoninic acid (BCA) assay.<sup>[11]</sup> As a result, two ( $\pm$  0.8) tetrakisNTA were bound to one  $\alpha$ N His<sub>6</sub>-proteasome complex, implying that one tetrakisNTA moiety is attached at each entrance of the proteasome. For the  $\beta$ C His<sub>6</sub>-proteasome, stoichiometries of 1:3 ( $\pm$  0.2) were deter-

mined. This higher labeling ratio can be explained by less-densely clustered histidine tags on the  $\beta$ C His<sub>6</sub>-proteasome.<sup>[8]</sup>

To provide evidence for the specificity of the MCH–His-tag interaction, *E. coli* cell lysates with  $\approx$  4300 different gene products<sup>[12]</sup> were incubated with tetrakisNTA (ATTO565) and analyzed by native-PAGE and fluorescence imaging (Figure 2). Comparison with isolated  $\alpha$ N or  $\beta$ C His<sub>6</sub>-protea-

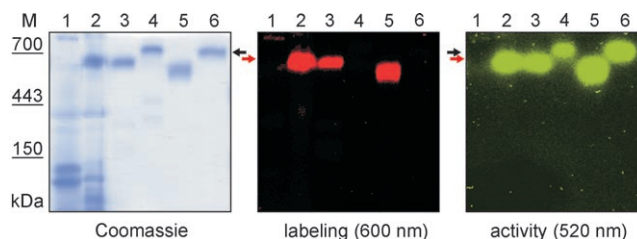


**Figure 2.** Specific labeling of 20S proteasomes within a complete cell lysate analyzed by native-PAGE and fluorescence imaging. Cell lysates (140  $\mu$ g *E. coli* proteins) or isolated 20S proteasomes (4  $\mu$ g in buffer solution A, see the Experimental Section) were incubated with tetrakisNTA (ATTO565) (17.1 pmol in lanes 1, 2, 3, and 5). Cell lysate without (lane 1) and with expression (lane 2) of  $\alpha$ N His<sub>6</sub>-proteasomes. Labeled and unlabeled  $\alpha$ N (lanes 3 and 4) as well as  $\beta$ C His<sub>6</sub>-proteasomes (lanes 5 and 6). Proteins were stained by coomassie brilliant blue G250 (left). TetrakisNTA (ATTO565) was detected at  $\lambda_{em}$  600 nm (middle). The activity of 20S proteasomes was monitored at  $\lambda_{em}$  520 nm by an overlay assay with Suc-LLVT-AMC (100  $\mu$ M; right). Black arrow and red arrow: unlabeled and labeled 20S proteasomes, respectively. M = molecular-weight marker, Suc = succinyl.

somes indicates that the fluorescent bands at  $\approx$  700 kDa (red arrow) correspond to labeled 20S proteasomes, which run slightly faster than unlabeled complexes (black arrow) because of the additional negative charges of the fluorescent MCHs. No labeling could be observed in cell lysates without expression of recombinant 20S proteasomes, demonstrating the high selectivity and specificity.

To investigate the peptidase activity of the 20S proteasomes toward small fluorogenic substrates, an in-gel-substrate overlay assay was performed by using Suc-LLVT-AMC.<sup>[13]</sup> Proteolytic cleavage of this nonfluorescent peptide leads to the release of fluorescent amino-4-methylcoumarin (AMC).<sup>[14]</sup> Fluorescence imaging of the overlaid gel shows that both the free and the labeled complexed proteasomes are active, and that the association of the MCHs has no significant influence on the peptidase activity of the archaeal proteasomes toward peptidic substrates. These findings are in agreement with the observation that the packing of the N-terminal tails of the  $\alpha$  subunits does not affect the entry of small peptides into the degradation chamber.<sup>[5]</sup>

The overlay assay only shows activity of single peptidase sites. Proteins have to be used as substrates to investigate the processive proteolytic activity of the proteasomes. Therefore, the influence of the MCHs on the degradation of fluorescein-labeled casein by the 20S proteasome was studied (Figure 3). Cleavage between fluorescein molecules attached to the casein leads to an increase in the fluorescence signal,<sup>[14]</sup> thus allowing the direct comparison of the activities of the free and complexed 20S proteasomes. Both recombinant 20S protea-

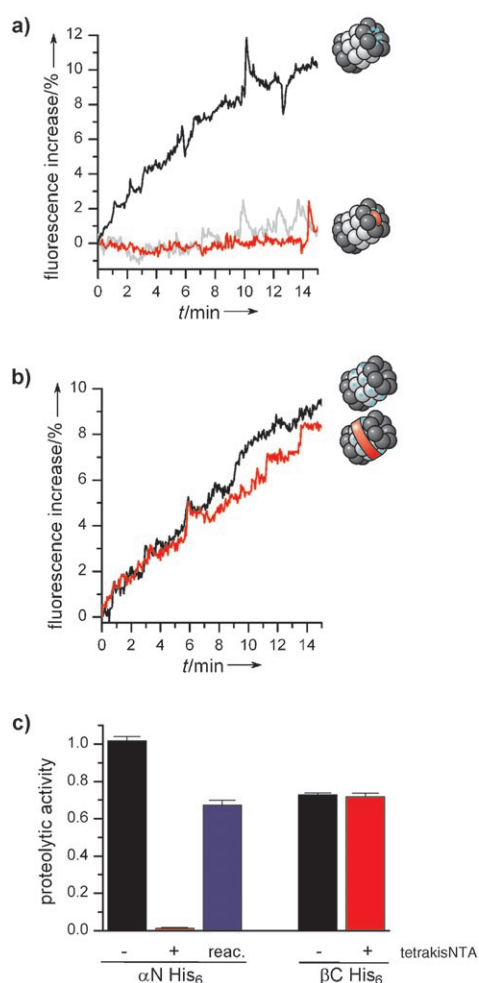


**Figure 3.** Real-time degradation of fluorescein-labeled casein (100 nm) by 20S proteasomes (10 nm) in buffer solution A at 60°C. a) Activity of the  $\alpha$ N His<sub>6</sub>-proteasome before (black trace) and after incubation with tetrakisNTA (140 nm; red trace) compared with the equilibrated fluorescein-labeled casein (gray trace). b) Activity of the  $\beta$ C His<sub>6</sub>-proteasome before (black trace) and after incubation with tetrakisNTA (10  $\mu$ M; red trace). c) Proteolytic activities of the recombinant 20S proteasomes with (red column) and without (black columns) tetrakisNTA, as well as activity of the reactivated  $\alpha$ N His<sub>6</sub>-proteasome after treatment with 50 mM imidazole (blue column).

somes have comparable activities (Figure 3, black traces and columns). However, after incubation with tetrakisNTA, the activity of the  $\alpha$ N His<sub>6</sub>-proteasomes is completely blocked, whereas the activity of the  $\beta$ C His<sub>6</sub>-proteasomes is not even affected by a 1000-fold molar excess of tetrakisNTA (red traces and columns). These results indicate that binding of the MCHs to the histidine tags at the entrances leads to a specific and complete blockage of protein substrate entry into the degradation machinery.

Apparently, binding of the MCH leads to the organization of the His-tagged N-terminal tails near the entrances to the degradation chamber, thereby inhibiting processive protein degradation. In the absence of nickel (II) ions and/or the presence of EDTA<sup>2-</sup>, the MCHs did not influence the proteolytic activity of the  $\alpha$ N His<sub>6</sub>-proteasome, demonstrating specific binding and full enzyme control. Imidazole

competes in binding against the His tags and can be used to reactivate the blocked proteasomes. Removal of the synthetic gatekeeper and isolation of the free  $\alpha$ N His<sub>6</sub>-proteasomes were performed by gel filtration (Figure 1c). The isolated, reactivated  $\alpha$ N His<sub>6</sub>-proteasomes show 70–80% of the original proteolytic activity, which nicely corresponds to the amount of uncomplexed proteasome obtained after gel filtration (Figure 3c). Therefore, inactivation of the 20S proteasome by the MCH is completely reversible, and the inherent processive proteolytic activity of the 20S proteasome is not affected by the complexation/decomplexation processes.

In conclusion, based on the nanomolar and highly specific binding properties, tetrakisNTA is a versatile tool for specific protein labeling even within the entire cell lysate. The high stability of the MCH–His-tag interaction allows the visualization and straightforward quantification of recombinant proteins by native-PAGE and fluorescence imaging. The reversible inhibition of the  $\alpha$ N His<sub>6</sub>-proteasome by tetrakisNTA for proteinaceous substrates demonstrates that the MCH can also be applied for the specific control and designed manipulation of macromolecular machines. The high specificity and binding affinity would, in principle, allow for labeling in vivo and inactivation of the 20S proteasome, which, based on its central role in numerous cellular processes, would be of great and general interest.

## Experimental Section

**Multivalent chelator head (MCH):** The tetrakisNTA was synthesized as described.<sup>[9]</sup> Carboxyfluorescein- (Fluka) or ATTO565-*N*-hydroxy-succinimide ester (ATTO-TEC) were coupled to the amino groups of the MCH in *N,N*-dimethylformamide (DMF). Purification of the fluorescent MCH was performed by reversed-phase C<sub>18</sub> HPLC, followed by loading the MCH with nickel(II) ions. The excess of nickel(II) ions was removed by anion-exchange chromatography (HiTrap Q, GE Healthcare). The tetrakisNTA concentration was determined by the absorption of the attached fluorophore.

**20S proteasomes:** The expression and purification of the recombinant 20S proteasomes was carried out as previously described.<sup>[7,8]</sup> For stable complex formation with the MCH, the 20S proteasome was incubated with a 10-fold molar excess of tetrakisNTA for 3 h on ice in buffer solution A (20 mM HEPES, 150 mM NaCl, pH 7.5). HEPES = *N*-2-hydroxyethylpiperazine-*N'*-2-ethanesulfonic acid.

**Gel filtration studies:** For the gel filtration, a Superose 6 PC 3.2 column (GE Healthcare) was equilibrated in buffer solution A with a flow rate of 50  $\mu$ L min<sup>-1</sup> at 10°C. A 50- $\mu$ L portion of 20S proteasome (0.8  $\mu$ M) in buffer solution A was added. To remove the tetrakisNTA from the 20S proteasome, the labeled proteasomes were incubated with imidazole (50 mM) in buffer solution A for 0.5 h on ice. The reactivated 20S proteasomes were isolated by gel filtration with imidazole (50 mM) in buffer solution A.

**Native-PAGE:** The native-PAGE as well as the substrate overlay assay were performed essentially as outlined by using a stacking gel with 3.5% polyacrylamide.<sup>[13]</sup> The EDTA<sup>2-</sup> concentration was reduced to 100  $\mu$ M to prevent interference with the MCH–His-tag interaction. Cell lysates with 140  $\mu$ g of *E. coli* proteins as well as 4  $\mu$ g of purified  $\alpha$ N and  $\beta$ C His<sub>6</sub>-proteasomes with and without fluorescent tetrakisNTA (17.1 pmol) in buffer solution A were loaded to the gel. After electrophoresis, the gel was overlaid with Suc-LLVT-AMC (100  $\mu$ M; Bachem) in Tris-HCl buffer solution (Tris (30 mM), MgCl<sub>2</sub> (5 mM), KCl (10 mM), DTT (0.5 mM); pH 7.8) for 20 min at 37°C to

investigate the activities of the 20S proteasomes. Tris = tris(hydroxymethyl)aminomethane, DTT = 1,4-dithiothreitol.

Degradation of fluorescein-labeled casein: The activities of the labeled and unlabeled 20S proteasomes were determined as published previously.<sup>[7,14]</sup> For labeling, a 14- or 1000-fold molar excess of the tetraakisNTA was used. The 20S proteasomes were added to a final concentration of 10 nM to a 100 nM solution of fluorescein-labeled casein in buffer solution A at 60°C. The fluorescence increase was monitored over 15 min at 495 nm.

Received: February 17, 2006

Published online: July 21, 2006

**Keywords:** biotechnology · fluorescence · inhibitors · protein engineering · proteomics

- [1] a) D. Voges, P. Zwickl, W. Baumeister, *Annu. Rev. Biochem.* **1999**, 68, 1015; b) A. L. Goldberg, *Nature* **2003**, 426, 895; c) M. Groll, M. Bochtler, H. Brandstetter, T. Clausen, R. Huber, *ChemBioChem* **2005**, 6, 222; d) A. Ciechanover, *Angew. Chem.* **2005**, 117, 6095; *Angew. Chem. Int. Ed.* **2005**, 44, 5944; ; e) A. Hershko, *Angew. Chem.* **2005**, 117, 6082; *Angew. Chem. Int. Ed.* **2005**, 44, 5932.
- [2] a) M. Groll, L. Ditzel, J. Löwe, D. Stock, M. Bochtler, H. D. Bartunik, R. Huber, *Nature* **1997**, 386, 463; b) M. Groll, M. Bajorek, A. Kohler, L. Moroder, D. M. Rubin, R. Huber, M. H. Glickman, D. Finley, *Nat. Struct. Biol.* **2000**, 7, 1062.
- [3] A. Forster, F. G. Whitby, C. P. Hill, *EMBO J.* **2003**, 22, 4356.
- [4] a) M. Groll, H. Brandstetter, H. Bartunik, G. Bourenkow, R. Huber, *J. Mol. Biol.* **2003**, 327, 75; b) F. G. Whitby, E. I. Masters, L. Kramer, J. R. Knowlton, Y. Yao, C. C. Wang, C. P. Hill, *Nature* **2000**, 408, 115; c) M. Groll, R. Huber, *Int. J. Biochem. Cell Biol.* **2003**, 35, 606.
- [5] D. M. Smith, G. Kafri, Y. Cheng, D. Ng, T. Walz, A. L. Goldberg, *Mol. Cell* **2005**, 20, 687.
- [6] a) J. Löwe, D. Stock, B. Jap, P. Zwickl, W. Baumeister, R. Huber, *Science* **1995**, 268, 533; b) W. Baumeister, A. Lupas, *Curr. Opin. Struct. Biol.* **1997**, 7, 273.
- [7] S. Hutschenreiter, A. Tinazli, K. Model, R. Tampé, *EMBO J.* **2004**, 23, 2488.
- [8] A. Thess, S. Hutschenreiter, M. Hofmann, R. Tampé, W. Baumeister, R. Guckenberger, *J. Biol. Chem.* **2002**, 277, 36321.
- [9] S. Lata, A. Reichel, R. Brock, R. Tampé, J. Piehler, *J. Am. Chem. Soc.* **2005**, 127, 10205.
- [10] C. van der Does, C. Presenti, K. Schulze, S. Dinkelaker, R. Tampé, *J. Biol. Chem.* **2006**, 281, 5694.
- [11] P. K. Smith, R. I. Krohn, G. T. Hermanson, A. K. Mallia, F. H. Gartner, E. K. Provenzano, E. K. Fujimoto, N. M. Goeke, B. J. Olson, D. C. Klenk, *Anal. Biochem.* **1985**, 150, 76.
- [12] F. R. Blattner, G. Plunkett, 3rd, C. A. Bloch, N. T. Perna, V. Burland, M. Riley, J. Collado-Vides, J. D. Glasner, C. K. Rode, G. F. Mayhew, J. Gregor, N. W. Davis, H. A. Kirkpatrick, M. A. Goeden, D. J. Rose, B. Mau, Y. Shao, *Science* **1997**, 277, 1453.
- [13] S. Hua, W. Y. To, T. T. Nguyen, M. L. Wong, C. C. Wang, *Mol. Biochem. Parasitol.* **1996**, 78, 33.
- [14] T. N. Akopian, A. F. Kisselev, A. L. Goldberg, *J. Biol. Chem.* **1997**, 272, 1791.